

High resolution Mapping of Agricultural Water Productivity using SEBAL in a cultivated African Catchment, Tanzania

D. Nyolei^a, M. Nsaali^{ab}, V. Minaya^a, A. van Griensven^{a/d}, B. Mbilinyi^c, J. Diels^b, T. Hessels^d, F. Kahimba^c.

^a Vrije Universiteit Brussels (VUB), Department of Hydrology and Hydraulic Engineering, Belgium

^b Katholieke Universiteit Leuven, Faculty of Bioscience Engineering, Belgium

^c Sokoine University of Agriculture, Soil Water Management Research Programme, Tanzania

^d IHE-Delft Institution for water education, Netherlands

Abstract

The application of remote sensing techniques for WP_{ET} mapping in data scarce regions is gaining more recognition since it can cover large areas with minimal field observations. Important concerns are the generation of high-resolution WP_{ET} maps and addressing the question on how accurate the results are. This study aims at high resolution (10m) mapping and evaluation of the spatial variability of biomass, yield, ET and WP_{ET} in the Makanya river catchment using the automated Surface Energy Balance Algorithm for Land (pySEBAL) with SENTINEL-2 and LANDSAT-8 images, local land use map and locally calibrated leaf area index (LAI) inputs. A coupled phenological variability and supervised classification approach on high resolution images generated a high accuracy LULC layer which was used to map the WP_{ET} in the agricultural lands. The pySEBAL results were evaluated in view of local information on crop yields, water allocation and agricultural management practices in the different agro-ecological zones within the catchment. Calibration of high-resolution satellite LAI generated products with error estimates within acceptable levels of uncertainty. The simulated crop yields were in agreement with reported crop yields. The results showed relatively high WP_{ET} in the highlands and low WP_{ET} in the midland and lowland areas of the catchment. The latter was attributed to high transmission losses, low irrigation efficiencies, poor agricultural practices and pest/disease attack. When applying SEBAL in African cultivated catchments, it is highly recommended to use SENTINEL-2 data in addition to LANDSAT-8, and to use local information, especially for the ground truthing of land use maps, phenology, crop practices and crop yields.

Keywords: evapotranspiration, Makanya, SEBAL, remote sensing, water efficiency, water productivity.

1. Introduction

Population growth imposes a steady increase in demand for food production around the world, which in turn puts a lot of pressure on the limited resources (Mancosu et al., 2015; Gerland et al., 2014). Particularly in sub-Saharan Africa, a region that will reach 25% of the world's projected population by 2050 (Gerland et al., 2014), water for agriculture and the availability of arable land are becoming increasingly scarce (Rockström and Falkenmark, 2015). Studies in the region have announced a water crisis with a critical and continuous reduction in freshwater quantity and quality exacerbated by climate change effects (Freitas, 2013; Pickering and Davis, 2012; Kula et al., 2013). A change of strategies in the current water resources management should include better and more efficient field management practices (Rockström and Falkenmark, 2015) in order to alleviate the water stress in sub-Saharan Africa thus improving agricultural water productivity (WP_{ET}). Most farming communities rely on rainfed agriculture for their livelihoods and unless improvements in WP_{ET} are made, projections in the crop water consumption will increase by 70% - 90% by 2050 under the current practices (de Fraiture et al., 2006).

Agricultural Water Productivity (WP) is defined as the crop produce derived from a specific volume of water regardless of its source whereas Agricultural Water Productivity (WP_{ET}) is defined as the crop yield derived from a specific volume of water evapotranspired (Perry et al., 2009; Kijne et al., 2003). For this study we will limit ourselves to Agricultural Water Productivity (WP_{ET}). In semi-arid regions, crops consume less than 30% of the rainfall, up to 50% is lost through soil evaporation and the rest flows as runoff and recharges groundwater (Rockström and Falkenmark, 2015). Farms that are near rivers can benefit from extra water supply through irrigation strategies while for distant farms this might be impractical. Mapping WP_{ET} at catchment scale, can help to identify areas with good and poor water management practices, assess effectiveness of the agricultural practices and evaluate the efficiency of rainfed and irrigated systems (Zwart et al., 2010). By carrying out WP_{ET} mapping, areas of low WP_{ET} can be spatially highlighted and used as focus for improvements by carrying out better land and water management practices (Cai and Sharma, 2010).

With a relatively stable, high population growth rate over the last decade that has been reported to be averaging between 6%–7% per annum (World Bank 2016), Tanzania has also exponentially reduced the renewable internal freshwater resource from 7862 m³ per capita estimated in 1962 to

1621 m³ per capita in 2014 (World Bank Database 1962-2014). In addition, the water resource in Tanzania is unequally distributed both spatially and temporally and therefore threatening the agricultural development and economic growth (URT, 2007). In the context of WP_{ET}, it is important to know the effective uses of water under the current agricultural practices and aim for solutions for crop yield improvement under water stress conditions. Makurira (2010) estimated the WP_{ET} for crops at field scale; however, little research has been done on the quantification at catchment level especially with the recent improvement in the spatial and temporal resolutions of satellite images. Increasing water productivity especially at catchment scale is key for improved water management through sustainable agriculture, food security and healthy ecosystem functioning. The ultimate goal is that cultivation practices meet the present and future challenges of agricultural water resource management at both field and catchment scales. Mapping water productivity at catchment scale however comes with the challenge of obtaining complete products for use to achieve the desired temporal resolutions due to cloud cover interference. Local validation of the catchment products has also been a challenge due to difficulties in implementing them along with high costs involved of obtaining local data to assist with producing high accuracy catchment products. Whenever field measurements are available, upscaling them to catchments has been difficult due to the nature of high spatial variability in many catchments.

The use of remote sensing data to determine actual evapotranspiration for irrigation management started back in the 1980's (Jackson, 1984; Jackson et al., 1981; Till and Bos, 1985; Menenti et al., 1989). However, operational algorithms were not available at that time. Later, Surface Energy Balance models were developed for using remote sensing to map evapotranspiration at different spatial scales (Bastiaanssen et al., 1998; Stewart et al., 1999; Choudhury et al., 1993; Rango and Shalaby, 1998). The Surface Energy Balance Index (SEBI) is an early example which is based on the contrast between dry and wet regions by deriving evapotranspiration from evaporative fraction (Choudhury and Menenti, 1993). Based on this principle, the Surface Energy Balance Algorithm for Land (SEBAL) was developed to map different aspects of the hydrological cycle and therefore to estimate the actual crop water consumption (Bastiaanssen et al., 1998). The SEBI model was then improved with the introduction of a simplified version, called the Simplified Surface Energy Balance Index (S-SEBI) (Roerink et al. 2000). In this algorithm, partitioning of available energy into sensible and latent heat fluxes was successfully achieved by establishing a contrast between the maximum and minimum surface temperature for dry and wet conditions through the reflectance

(albedo). Another modified form of the SEBI was later developed and named the Surface Energy Balance System (SEBS) by Su, Z (2002). SEBS estimates sensible and latent heat fluxes from satellite data and routinely available meteorological data. Most recently, the Mapping Evapotranspiration at high Resolution with Internalized Calibration (METRIC) algorithm (Allen et al. 2007) was introduced which is a modified version of SEBAL. The METRIC algorithm includes the integration of reference ET as computed from ground-based weather data. SEBAL has been identified as the most promising approach currently available to estimate evapotranspiration. SEBAL can be used without prior knowledge of the existing field conditions such as the soils, existing crops and management practices (Bastiaanssen et al., 2005). It also has the advantage of requiring minimum ground weather data, making it useful for places with limited data such as in some developing countries. With little ground data available, SEBAL can compute the surface energy balance components, both at local and regional scales. The innovation part in SEBAL is that the surface energy balance modelling uses a near-surface temperature gradient which is indexed to radiometric surface temperature. This has eliminated the need for absolute surface temperature calibration, which has been a major challenge with operational satellite ET (Allen et al. 2011). SEBAL has been widely applied since its creation, around 303 articles and review publications have been identified (Scopus Database until July 2017); however just a few have been carried out in the sub-Saharan Africa (Kiptala et al., 2014; Andam-Akorful et al., 2014). This method has been verified in several climatic conditions for both field and catchment scales with typical accuracy at field scale of 85% and 95% for daily and seasonal scales, respectively, in over 30 countries worldwide. SEBAL has been used extensively for ET estimation and most recently it has been further improved through the pySEBAL system, a complete automated user-friendly python-based system, to include biomass estimation and mapping for different land use classes as well as fields with different irrigation methods at catchment scale (Ahmad et al., 2006; Jarman et al., 2011, 2013; Jarmin and Meijninger, 2012). Most recently, the Sentinel family of remote sensing images has been introduced with images with as high as 10-meter resolution. Products from interpretation of these images are expected to provide better spatio-temporal resolution results which when coupled with other images could provide even more valuable information for both local and regional studies. In this study, we investigate the joint use of Sentinel-2 and LANDSAT-8 images for high resolution (10 m) ET and WP_{ET} mapping using

SEBAL in a cultivated tropical catchment in Tanzania. Few studies have been evaluating the use of Energy Balance Models in cultivated Sub-Saharan tropical catchments.

Validation of estimated ET results from SEBAL and other RS algorithms is usually achieved using field-based ET measurement techniques. Most of these ET measurement techniques are quite expensive to implement and require highly skilled and experienced personnel to operate. They also require a lot of care during installation and maintenance. Some of the known and widely used ET measurement techniques that are also used for validation of remote sensing ET estimates are; the Bowen ratio Energy Balance (BREB), soil water balance, Eddy covariance, lysimeters, mass balance over large areas, Scintillometers, sap-flow. When correctly installed, operated and ET computations correctly done, accurate sub-hourly ET measurements could be achieved of about 5% for lysimeters, 10% for BREB systems and soil water balance techniques, 10-15% for eddy covariance and Scintillometers (Allen et al 2011a).

This paper presents the application of the recently introduced Sentinel-2 images and the newly developed pySEBAL tool for Landsat images to easily map biomass, yield, LAI, and ET in the Makanya catchment in Tanzania. It also presents a methodology of applying data fusion techniques of Landsat-8 and Sentinel -2 aimed at downscaling the Landsat products to spatial resolutions of 10-meters, together with field data and local information on water allocation and water management practices. The main objectives of this study were (1) to map and evaluate the spatial variation of biomass, LAI, yield, ET and WP_{ET} in the different agro-ecological zones using the Sentinel-2 images and the SEBAL model through its newly developed pySEBAL system for Landsat images, (2) to evaluate the results using local information, and (3) to discuss the water management practices by linking it to the water and field management practices.

2. Methodology

2.1 Study area

2.1.1 Location

The Makanya catchment (375 km²) lies within the Pangani river basin, located in the north-eastern part of Tanzania. The Makanya River flows between two mountain ridges in the South Pare Mountains in the Kilimanjaro region of Tanzania (Figure 1).

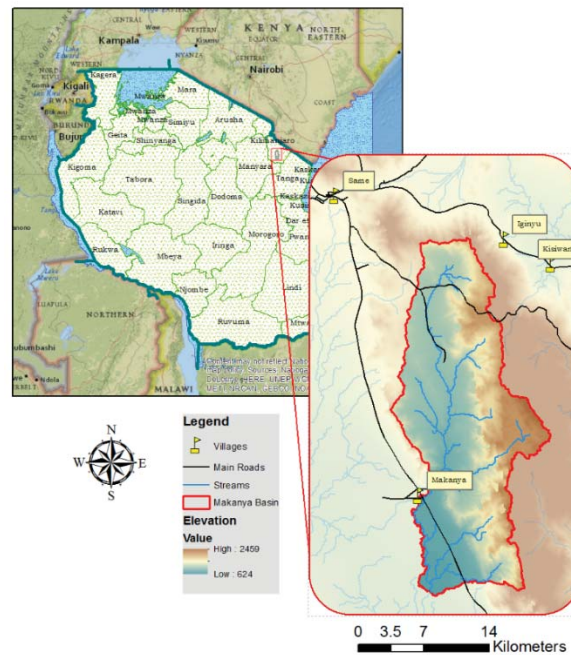


Figure 1: Location of the Makanya river catchment

2.1.2 Climate

The climate is dry sub-humid to semi-arid with a bimodal rainfall pattern having a longer rainy season between March and June (*Masika*), and a shorter rainy season between October and December (*Vuli*) (Enfors and Gordon 2007). The average annual rainfall in the Makanya catchment ranges from 500-800 mm per annum (Mul, 2009). The mean minimum temperature ranges from 16 to 18°C and mean maximum temperature ranges from 26 to 32°C (Mutiro et al., 2006). The potential evaporation during the short rain season varies between 1120 and 1610 mm and between 870 and 1325 mm during long rain season (Kinoti et al., 2010).

2.1.3 Agro-ecological Zones

Based on elevation, the catchment stretches across three agro-ecological zones; highlands, midlands and lowlands, whereby the climate, ecology and demographics vary among these three zones. Highlands (>1350 m a.s.l.) are characterized by having water availability throughout the year, agriculture and agroforestry as the main land use, and a high population density. Midlands (750 – 1350 m a.s.l.) are distinguished by having hotter and drier areas compared to the highlands, landscape is dominated by cropland and bushland for grazing, small-scale farming as well as livestock keeping. Lowlands (< 750 m.a.s.l.) exhibit very low rainfall, and therefore crops depend on spate irrigation from flash floods, which occurs a few times in the year. Farmers experience

crop failures due to water shortages making livestock the most important source of livelihood (Enfors and Gordon, 2007).

2.1.4 Water allocation practices

In the highlands and midlands, the river water is diverted mainly for supplementary irrigation during the wet and dry seasons. This water is also used for domestic and livestock uses. In these areas, farmers make use of micro dams constructed for purposes of night storage and providing a hydraulic head to supply the downstream farmers in the midlands. Lowland farmers have jointly developed a system of diversion canals that are used to divert flood waters into the crop fields. The catchment has over 100 hand-dug unlined irrigation furrows mostly made from rudimentary materials. Each of the furrows supplies water to a farm land ranging from 0.5 to 400 ha. Total water losses in the Makanya catchment irrigation systems have been recorded to be very high, ranging between 75% and 85% (Mul et al., 2011).

Existing agreements among irrigators specify a water sharing system on a rotational basis at different spatial scales within the same sub-catchment. In addition, there is a specific agreement at sub-catchment level between the highlands and the midlands where the highlands are allowed to use the water for irrigation only during the day. At night, water is released to the midlands where it can be stored in micro-dams for midlands to use it during the next day. There are no water sharing agreements in the lowlands of the Makanya catchment. The water sharing arrangements are negotiated through social networks of the smallholder farmers and are therefore built on the social ties between the communities up to sub-catchment scale, without the intervention of the national authorities.

2.2 Data collection

2.2.1 Remote sensing data

Landsat 8 OLI and Sentinel-2 images were used as the remote sensing data for this study. This decision was arrived at as the Sentinel products provided the highest spatial resolution of free products for land cover, Leaf Area Index (LAI), Vegetation Indices (VI), Fraction of Absorbed Photosynthetically Radiation (FAPAR), Biomass and yield mapping. Landsat on the other hand provides the highest spatial resolution of free thermal band, which is critical for ET estimation efforts in small to large areas. Further improvements on the resolution of the thermal band is also possible through thermal sharpening using other higher resolution bands within this satellite

platform. In this study, the spatial resolution of the thermal band was improved through thermal sharpening to match the spatial resolution of 30m of the other Landsat products. This thermal sharpening procedure is built within the pySEBAL system used for our study.

2.2.2 Meteorological data

Meteorological data that is also required for ET estimation from SEBAL were obtained from the local weather station of the Tanzania Meteorological Agency in Same town. More meteorological data was also obtained from a weather station within the catchment that had been installed during a previous research project.

The weather data used in this study were; instantaneous air temperature, average air temperature over 24 hours, instantaneous relative humidity, average relative humidity over 24 hours, instantaneous wind speed at two (2) meter height, average wind speed over 24 hours, instantaneous solar radiation and average solar radiation over 24 hours.

2.2.3 Ground measurements

A ground truthing campaign was carried out in the Makanya catchment during different times of the year 2017 for land use - land cover (LULC) characterization and classification along with water use through irrigation and crops yields obtained from the farms. The campaign was carried out by taking GPS coordinates for the different LULC categories. Detailed land use patterns and crop characteristics were also recorded as well as the irrigation frequency, crop yield, crop rotation and crop growth cycles, observations and interviewing farmers. During the field campaign, a heterogeneous landscape was observed, with patches of agriculture and sparse houses along the catchment. The crops in highlands are a mixture of banana, coffee and fruit trees; however, the main crop cultivated in the three agro-ecological zones is maize, which is mainly used for household consumption. The crop maturity depends mainly on the crop variety, micro climate and water availability. The growth stages, health conditions and humidity of the agricultural fields are highly variable within the catchment.

Leaf Area Index (LAI)

The SS1 Sunscan Canopy Analysis System (Delta-T Devices Ltd) was used for ground LAI measurements. This system uses two sensors, the BF5 sensor, which captures all incident radiation from the sun, and the Sunscan probe, which measures the total transmitted light through the

canopy. By acquiring the incident and transmitted radiation of the canopy, LAI is computed using a model developed by Campbell (1986) which also uses constants for Ellipsoidal Leaf Area Angle Distribution Parameter (ELADP) and Absorption (percentage of incident Photosynthetically Active Radiation (PAR) absorbed by the leaf) (Campbell 1990). Default values of Absorption = 0.85 and ELADP = 1.0 were used (Webb et al., 2016). The LAI was measured in maize fields under different growth stages over different parts of the catchment. These measurements were carried out in the second week of March in order to capture typical values of LAI of maize at different stages of growth. These LAI measurements were used to validate the Sentinel-2 and Landsat-pySEBAL generated RS products of LAI. High LAI variability from some field measurements came from heterogeneity in some fields. Human error when taking measurements was also a possible cause of the variability. Whenever possible, measurement values that appeared as outliers were rejected.

Selection of study fields

Five field sites with maize crops in their late stages were randomly selected for validation of the LAI estimated with remote sensing products (Table 1); however, no field sites were selected from the lowlands because during the field campaign none of the fields were at their late stage of growth. In these fields, a minimum of five (5) measurements of LAI were taken within each field that would later be used for validation of the RS products through the different pixel values in the fields. Other fields with maize at the mid or early stages were also selected for validation of the RS LAI products.

Table 1: Selected study fields with maize at different growth stages

Field	Location	Water Application	Latitude	Longitude	Average LAI	Remarks
A	Highlands	Rainfed	-4.21088	37.88592	0.99	Irrigated once after sowing, terraces, organic mulching
B	Highlands	Rainfed	-4.21192	37.88549	1.46	Terraces, organic mulching
C	Highlands	Irrigated	-4.20926	37.88659	2.32	Terraces, chemical fertilizers
D	Midlands	Irrigated	-4.22973	37.85413	1.20	Soil bunds, no fertilizer
E	Midlands	Irrigated	-4.22901	37.85194	1.70	No soil bunds, no fertilizer
F	Midlands	Irrigated	-4.23610	37.84399	1.38	Soil bunds, no fertilizer
G	Lowlands	Rainfed	-4.36959	37.82850	0.97	No soil bunds, no fertilizer
H	Lowlands	Rainfed	-4.37031	37.82482	0.63	No soil bunds, no fertilizer
I	Lowlands	Rainfed	-4.37059	37.82482	0.79	No soil bunds, no fertilizer

2.3 Biomass, yield, water use and water productivity mapping

The methods for biomass, yield, water use and WP_{ET} mapping using remote sensing are described in this section and consist of: i) LULC classification to delineate the agricultural area, ii) Actual ET mapping for the season using SEBAL, iii) Crop yield mapping calculated from biomass maps generated from Sentinel-2 and SEBAL products, and iv) Water productivity mapping considering the conversion factors.

2.3.1 Land Use -Land Cover (LULC) classification

Sentinel-2 images with resolution of 10 m were downloaded from the ESA Copernicus website. Cloud free Images or images with minimal cloud cover covering different times of the year from the wet to the dry season were downloaded to assist with accurate and efficient LULC interpretation. The Semi-Automatic Classification (SCP) tool developed for QGIS was used for image pre-processing which included radiometric and atmosphere correction, layer stacking and haze removal. This tool was also used to generate NDVI products for all the downloaded Sentinel-2 images. Interpretation of the NDVI products assisted with performing preliminary LULC classification where agricultural lands were mapped based on phenological variability while other classes such as forests, bare soil and settlements were identified based on their NDVI values. The products from this classification were later coupled with supervised classification using training data obtained from the ground truthing data and the maximum likelihood classifier. A total of 6 LULC classes were defined which included forest, shrubs, agriculture, bare soil, sisal plantation and settlements.

Accuracy assessment for the LULC classification

Accuracy of the produced LULC map was evaluated using ground truthing data as an independent reference data by overlaying the GPS points of the ground truth data on the LULC layer and evaluating the level of agreement. We then adopted the approach described by Olofsson et al. (2013) to estimate accuracy of the LULC classification. Using the SCP tool in QGIS an error matrix statistic was generated. This produced the errors of omission and commission for each LULC class, Producer's accuracy, User's accuracy, and Overall accuracy

2.3.2 Actual evapotranspiration mapping

The approach involved the use of remotely sensed data, a combination of LULC classification and actual ET computation for crops using the Surface Energy Balance Algorithm for Land (SEBAL).

The pySEBAL is a surface energy balance model comprising of twenty-five computational sub models that uses digital image data / satellite imagery to compute evapotranspiration (ET) and other land surface energy exchanges (Bastiaanssen et al., 1998). The PySEBAL is a version of the SEBAL algorithm that has been developed in Python, an open source platform that runs SEBAL through semi-automatic processing of selected satellite images (Hessels et al., 2017). It has been used for water use monitoring, water use efficiency, water productivity and planning purposes for various crops in several Asian and African countries (Cai et al., 2017). The PySEBAL model uses satellite images that allow calculations for atmospheric correction using empirical equations, DEM, meteorological and soil data characteristics. For this case study, an SRTM-DEM product downloaded from earthexplorer.usgs.gov was used and clipped to the size of the study area. Meteorological data, obtained from Same weather station, included instantaneous (hourly) and daily air temperature (°C), relative humidity (%), wind speed (m/s), height of measuring wind speed (m) and incoming solar radiation (W/m²).

Actual evapotranspiration by crops was determined using the SEBAL model. SEBAL calculates the energy balance using satellite (visible, infrared, and thermal infrared radiation) images as input as well as meteorological data such as humidity, wind speed, solar radiation and air temperature and soil variables. It solves the instantaneous energy balance and uses extrapolation to calculate daily evapotranspiration. The actual ET is obtained using the surface energy balance equation:

$$\lambda ET = R_n - H - G \dots\dots\dots \text{Equation 1}$$

where λET is the latent heat flux in the atmosphere boundary layer (W/m²), R_n is the net radiation (W/m²), H is the sensible heat flux (W/m²) and G is the soil heat flux (W/m²). The instantaneous ET flux is calculated for each pixel of the image as a “residual” of the surface energy budget equation and is expressed as the energy consumed by the evaporation process. A latent heat flux of 28 W/m² is equal to an evapotranspiration rate of 1 mm/d.

Satellite radiances are converted into land surface characteristics such as surface albedo, surface temperature and vegetation indices such as leaf area index (LAI), Normalized Difference

Vegetation Index (NDVI) and Soil Adjusted Vegetation Index (SAVI) which are used to compute the different fluxes in the energy balance equation. The net radiation (R_n) is computed by subtracting all outgoing radiant fluxes from all incoming radiant fluxes. The soil heat flux (G) is calculated as a G/R_n fraction using NDVI, surface temperature and surface albedo. Sensible heat flux (H) is computed using wind speed observations, estimated surface roughness and surface to air temperature differences that are obtained through calibration of hot ($\lambda ET=0$) and cold ($H=0$) pixels. The soil heat flux (G) and sensible heat flux (H) are then subtracted from the net radiation flux at the surface R_n to compute the residual energy available for evapotranspiration (λET). The instantaneous latent heat flux, λET is then converted into daily λET_{24} assuming a constant evaporative fraction (Λ) for 24 hours calculated from the instantaneous energy fluxes as observed in the satellite data as:

$$\Lambda = \frac{\lambda ET}{R_n - G} \dots \dots \dots \text{Equation 2}$$

The daily actual evapotranspiration can then be determined as:

$$ET = \frac{86,400 \times \Lambda \times (Rn_{24} - G_{24})}{\rho_w \times \lambda} \dots \dots \dots \text{Equation 3}$$

where Rn_{24} is the average net radiation for the day computed from raw products of instantaneous satellite spectral radiance, vegetation indices and satellite surface temperatures which are then expressed as average day estimates. G_{24} is the daily soil heat flux (W/m^2) which is computed from instantaneous satellite products of NDVI, surface temperature and surface albedo before converting them also to average day estimate, λ is the latent heat of vaporization used to convert the energy to mm of evaporation and is a function of temperature and ρ_w is the density of water (kg/m^3) (Singh et al., 2008).

SEBAL generates actual evapotranspiration (ET_a) maps in mm/day for each of the input satellite images. For this study, five cloud free Landsat images were obtained for the months of October, December, January, February and March. With these products, a seasonal polynomial fit was implemented to estimate the seasonal ET. Using the input meteorological data, it generates reference evapotranspiration (ET_o) maps. Crop coefficient (K_c) maps are then computed as a ratio of the ET_a and ET_o maps in the pySEBAL code. PySEBAL interpolates linearly among the K_c maps to generate daily K_c maps then calculates daily ET_a maps by multiplying each K_c image with

the corresponding ET_o value. The ET_a maps are then summed up for the user defined crop growing season to generate the seasonal ET_a map. For this research, a cropping period of 90 days was used for the season starting on 8th December 2016 to 8th March 2017 leaving out days before crop emergence.

2.3.3 Calibration and validation of Sentinel-2 and Landsat-8 LAI results

For this study, we were not able to implement any ET measurement and validation techniques. But as the Sentinel Application Platform (SNAP) and the pySEBAL calculates 10- and 30-meter resolution LAI respectively as an important intermediate step in the procedure to calculate ET and biomass, we chose to validate these products using field measurements of LAI. The ground measured LAI values in the selected study fields were used to validate the Sentinel-2 and Landsat-pySEBAL results of LAI at the time of satellite overpass by computing error estimates using standard and root mean-square errors and estimating the uncertainty of the LAI products.

2.3.4 Crop biomass and yield mapping

First the Landsat Biomass maps were generated by the pySEBAL tool in kg/ha/day, representing the dry biomass generated that day per hectare. The pySEBAL calculates biomass by first looking at the biomass that can be produced when there is always water available, and then multiplies this by constraining factors (heat, vapor and moisture stresses) which are obtained from meteorological data, potential ET and actual ET. These biomass products are therefore a function of the fraction of absorbed photosynthetically active Radiation (FAPAR), photosynthetically active Radiation (PAR) and the light use efficiency (LUE). Some of these parameters, especially those related to vegetation, such as the Fraction of Absorbed Photosynthetically Active Radiation (FAPAR) can also be generated from the biophysical processor built into the Sentinel Application Platform (SNAP) for Sentinel-2 and the pySEBAL for Landsat-8. LUE and LAI have been reported to have strong correlation making it possible to integrate LAI from both platforms together leading to downscaled LUE to produce high-resolution and improved LUE products. The high-resolution products of APAR and LUE were then used to generate the high-resolution, 10m, biomass products. From the daily biomass products, we applied a polynomial fit to generate monthly biomass which were later summed up to get biomass generated for the season. The season's biomass map was used to calculate the agricultural crop yield for the delineated agricultural areas by multiplying the biomass by a field computed average harvest index for maize of 0.47 for the

area under the assumption that maize is the most dominant crop in the catchment. This harvest index was obtained from the ratio between the biomass measured in the area and the average yields measured and what was reported by the farmers.

2.3.5 Water productivity mapping

WP_{ET} [kg/m^3] was obtained by dividing the crop productivity (agricultural yield) [kg/m^2] by the actual evapotranspiration expressed in [m^3/m^2].

$$WP_{ET} = \frac{\text{crop yield}}{ET_a} \dots\dots\dots \text{Equation 4}$$

3. Results and Discussion

3.1 Land Use Land Cover (LULC) Classification

The LULC map of 2017 for Makanya catchment (Figure 2) shows bushland (55%) as the dominant land cover class mainly in the highlands followed by agricultural areas at about 20% occurring mostly in highlands and midlands. The forests came at the third place and occurs mostly in the highland (Table 2). Bare soil (7%) covers a small area that occurs in small patches in the entire midland and lowland. Settlements also present a low percentage in the catchment although the area is characterized by small sparse houses in various parts of the catchment that were quite hard to visualize in the map except for the small market centers. The small patches of rocky areas known to be located on the peaks of the mountains were not classified because of their small size and the proximity to other classes such as bushland or forest that influence the visual identification and the precision in the training stage.

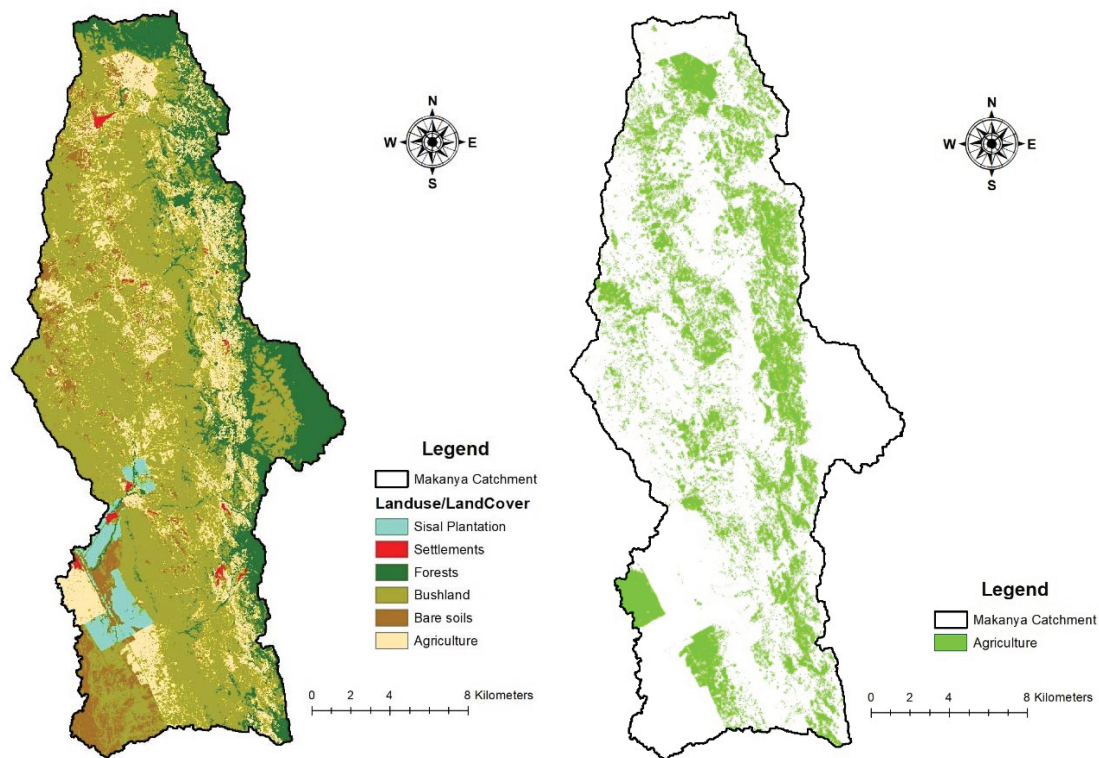


Figure 2. a) Land use map and b) Agricultural areas for the Makanya catchment

Table 2. Percentage of LULC classes for Makanya catchment.

LULC Class	Area (Ha)	Percentage (%)
Agriculture	7,446	20%
Bare soils	2,666	7%
Forests	5,759	15%
Settlement	142	1%
Bushland	20,587	55%
Sisal Plantation	918	2%
Total	37,518	100.0%

Tables 3 shows the results of accuracy assessment, in terms of omission error, commission error, producer's accuracy, user's accuracy and overall accuracy of LULC map. The results revealed an overall accuracy of 82%. Considering the categories accuracy, the LULC mapping provided different producer's and user's accuracy levels indicating different levels of omission and commission errors. High variability was however noted in the producer and user accuracy results

of the bushland. This variability was especially caused by some sisal plantations that have since been abandoned leaving the plantations to be filled with bushes. During classification these plantations are easily confused with bushland.

Table 3: Error matrix

Classified Data	Reference Data						Total	Area (ha)	Accuracy (%)		
	Ag	Bul	SP	St	BaS	Fr			Producer's	User's	Overall
Agriculture (Ag)	34	5	0	0	0	1	40	7,446	73.9	85.0	82.0
Bushland (Bul)	4	80	19	0	3	7	113	2,666	88.9	70.8	
Sisal plantation (SP)	7	4	137	3	0	19	170	5,759	86.2	80.6	
Settlement (St)	0	0	2	25	0	3	30	142	86.2	83.3	
Bare Soils (BaS)	1	0	0	0	22	0	23	20,587	88.0	95.7	
Forest (Fr)	0	1	1	1	0	72	75	918	70.6	96.0	
Total	46	90	159	29	25	102	451	37,518			

3.2 Leave Area Index (LAI)

Field measured LAI corresponded fairly well with the satellite estimated LAI in the midlands and lowlands, however, this was not the case in the highlands. Improved remote sensed LAI was therefore needed and could only be achieved through calibration. This was implemented by plotting and developing a model from the field measured and satellite estimated LAI from the field where the RS LAI best matched the field measurements as presented in figure 3 below. The equation from this relationship followed a near linear pattern that yielded an equation applied over the satellite LAI. This led to improved estimates of LAI for the entire catchment that better matched the field measured LAI values. satellite LAI values in the highlands were however still slightly higher than the ground measured values since the farms in the highlands are mainly small and strongly heterogenous as characterized by mixed vegetation especially with the presence agroforestry systems (trees on farms). The high LAI vegetation in the farms or around the small farms in the highlands contaminated the RS estimated maize LAI values. High LAI variance was also noted in the lowlands as not all the farms were cultivated during this season. During this season the rainfall amounts are usually quite low with no benefit of irrigation water therefore most farmers prefer not to farm leaving most of the agricultural lands bare or with small stacks of naturally

growing vegetation as they await the long rains. This also explains the reason for low ET values in the agricultural blocks in the lowlands. Few farmers however usually gamble and cultivate their farms during this season, and this explained the presence of slightly high LAI values from these farms.

The results of RS LAI showed a clear negative gradient from the highlands to the lowlands. The highlands, on average, receive and consume more water than the other zones thereby producing more biomass which explains the high LAI values observed in this zone. Despite the midlands receiving almost similar amount of rainfall as the lowland, higher LAI values were observed in the midlands. This was because the midlands benefited from supplementary irrigation leading to more biomass and in turn high LAI values. The lowlands receive the least amount of water thereby having the least seasonal water use, biomass as well as yields.

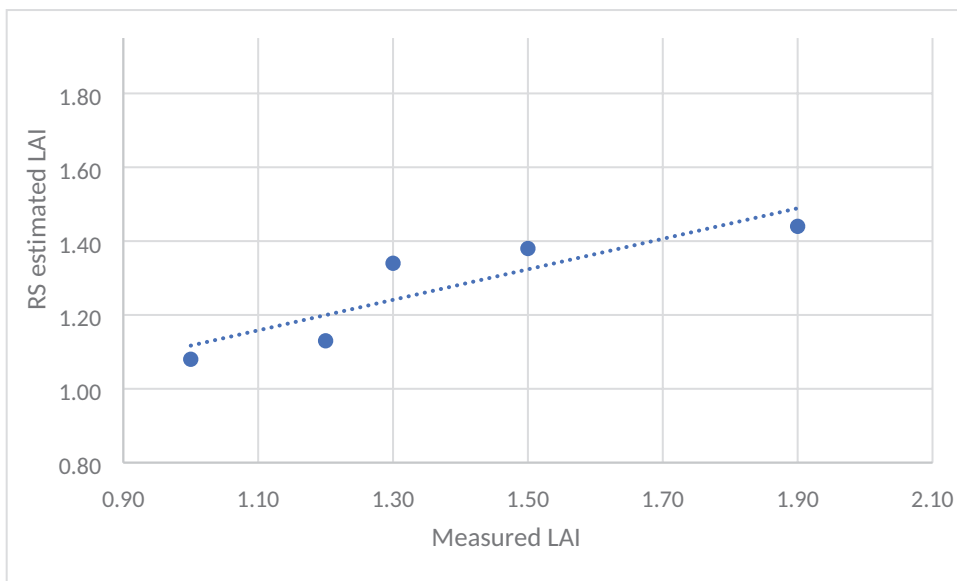


Figure 3: Field measured LAI plotted against remotely sensed LAI

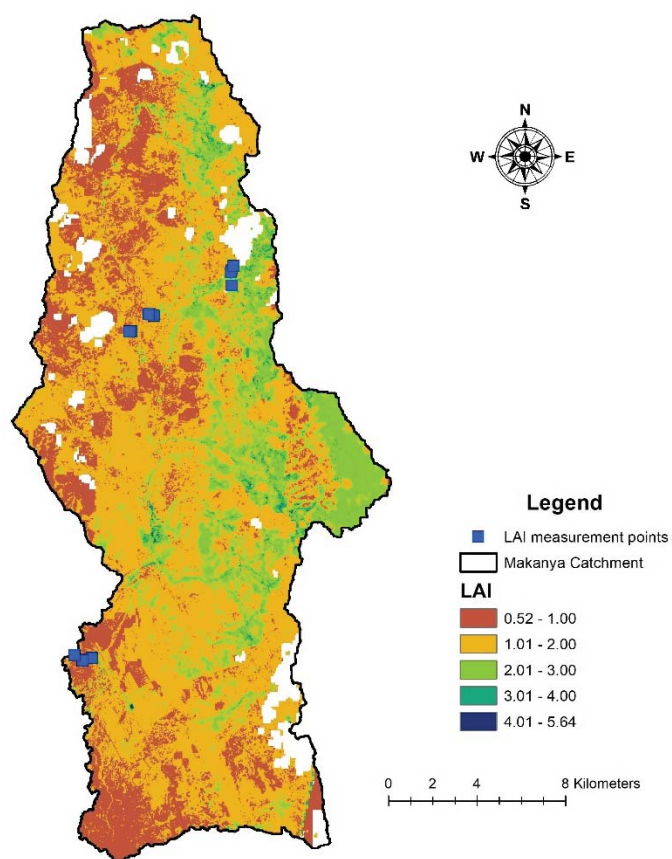


Figure 4. Leaf Area Index for the Makanya catchment in March 2017

Table 4: Sentinel-2 LAI Error estimates

Zones	Field	Standard Error	Ave. Standard Error	RMSE	Ave. RMSE
Highlands	A	0.317	0.183	0.245	0.134
	B	0.088		0.036	
	C	0.144		0.122	
Midlands	D	0.177	0.313	0.125	0.200
	E	0.589		0.340	
	F	0.174		0.134	
Lowlands	G	0.274	0.150	0.245	0.132
	H	0.044		0.036	
	I	0.132		0.114	

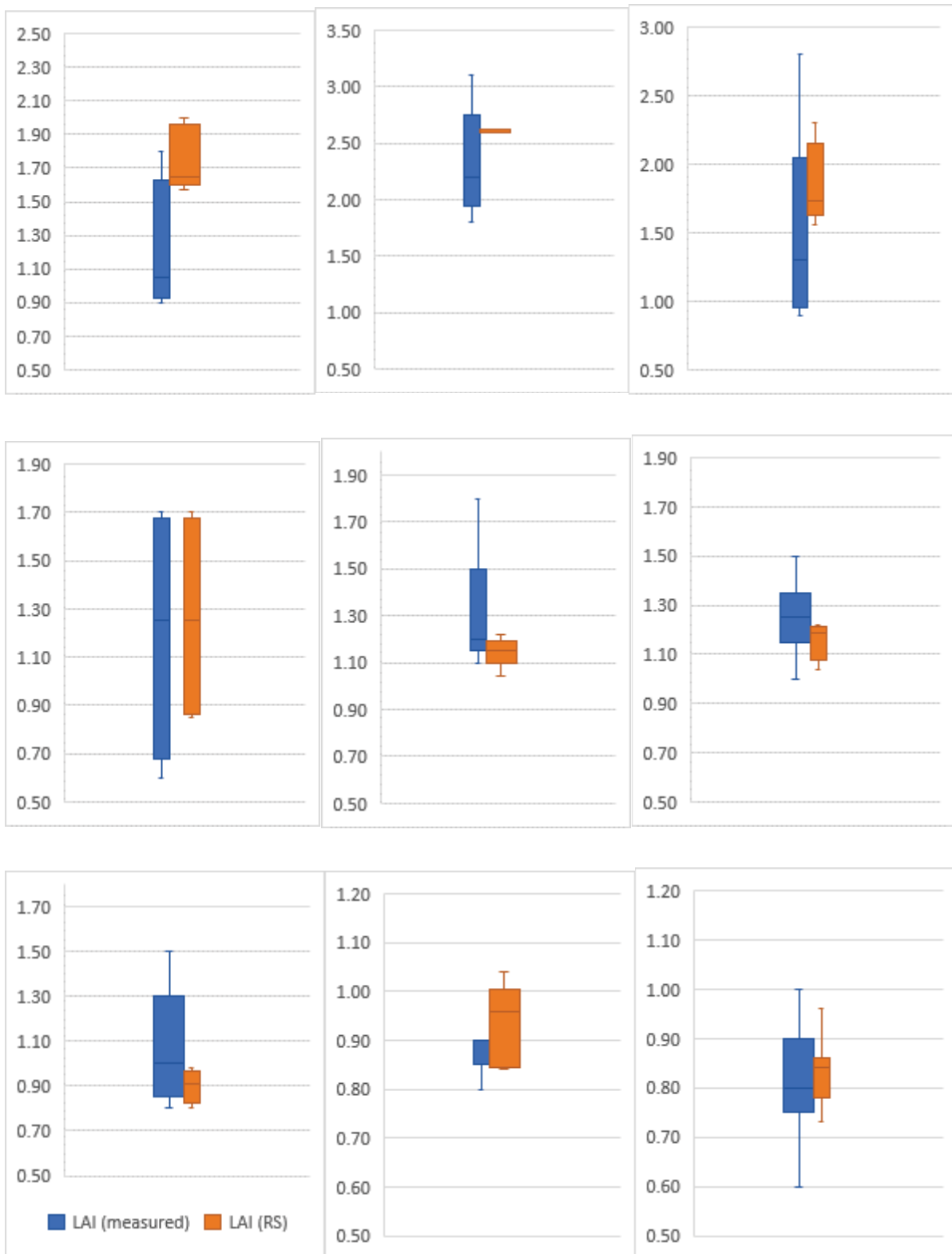


Figure 5. Leaf Area Index error estimates for the sample fields in the highlands (top), midlands (center) and lowlands (bottom)

While efforts were made to improve the accuracy remotely sensed LAI by minimizing on the errors, uncertainties from numerous sources could not be eliminated. Numerous sources of uncertainties exist, however, the commonly known sources include: (1) natural variability, (2) measurement error from in situ optical LAI devices, (3) human errors during field measurements, (4) spatial scale differences between the ground sampling footprint and the resolution of satellite imagery and (5) spatial averaging error in the aggregation process, and (6) GPS uncertainty. This research identified these common sources as having contributed to the uncertainty in the LAI results obtained. Quantification of the errors associated with all these sources along with propagation of uncertainty through to the final LAI products was however out of the scope of this study. We instead attempted to estimate the uncertainty based on the error estimates associated with LAI field measuring device, sampling uncertainty, satellite product radiometric and atmospheric calibration uncertainty and data processing approach by assuming that the errors were additive. The SS1 Sunscan Canopy Analysis System along with potential systematic biases due to data processing decisions are estimated to be 10–20% (Richardson et al. 2011). Sentinel-2 Level 1C Top-Of-Atmosphere reflectance products (L1C-TOA) have typical radiometric calibration uncertainty better than 3% with the worst-case, but rare, uncertainties being about 5% (Gascom et al. 2017, Kaan et al. 2016) while atmospheric corrected sentinel-2 products have uncertainty under 3% (Mannschatz et al. 2014). Sampling uncertainty is an additional source of uncertainty, but this is usually relatively small (Richardson et al. 2011). Together all these individual uncertainties add up to overall RS LAI uncertainty of 20-30%. In most of the fields where LAI measurements were taken, the standard error of the remotely sensed LAI were under 0.2. This demonstrated that the LAI estimates were well within acceptable limits making the products within the acceptable range of uncertainty.

Studies on LAI uncertainty propagation have shown that LAI errors under 0.3 present small to moderate uncertainty to Soil–Vegetation–Atmosphere models that are applied to simulate how vegetation affects the water balance and energy fluxes (Mannschatz et al. 2014). The results from this study are therefore expected to have small to moderate effects on the uncertainty of the ETa, Biomass, yield and WPET products coming out of this study.

3.3 Seasonal actual evapotranspiration (ET_a)

We assumed that the entire agriculture LULC was covered by maize crops. This was because maize was the dominant food crop grown by the farmers in the area. The seasonal average ET_a of maize crops in the agricultural areas for the period December 8th, 2016 to March 8th 2017 was 331 mm, with the pixel values ranging from 152 mm to 476 mm along with a standard deviation of 48 mm. The large seasonal ET range observed may be attributed to the different daily ET estimates for the different farms due to different growth stages of the maize crops and the presence of other crops such as bananas, coffee and fruits trees in agriculture lands. The different growth stages of the maize crops are common in the area especially during the Vuli season as the farmers don't all grow at the same time. Some farmers plant as early as mid-October while others grow as late as mid-December. In turn the water sharing arrangements in the midland area doesn't provide an efficient and effective system that allows for the practice of supplementary irrigation in an equitable manner. Farmers with large maize fields may sometimes irrigate a section of their fields before the reservoirs runs out of water with no possibility of getting more irrigation water in the following day to irrigate the remaining sections. This leads to highly varying ET estimates in sections that received irrigation water compared to those that didn't receive any water. This variation can also be explained by the presence of rainfed and irrigated farms in the catchment, especially in the midlands along with varying agricultural practices by the different farmers. The large seasonal ET range may also be attributed to the different agro-ecological zones in the catchment as observed in Figure 5 and the fact that not all the agriculture lands had crops during this season. The highlands displayed the highest ET_a with an average of 343 mm for the season, followed by the midlands with an average seasonal ET_a of 293 mm, and the lowlands averaging 241 mm (Figure 6).

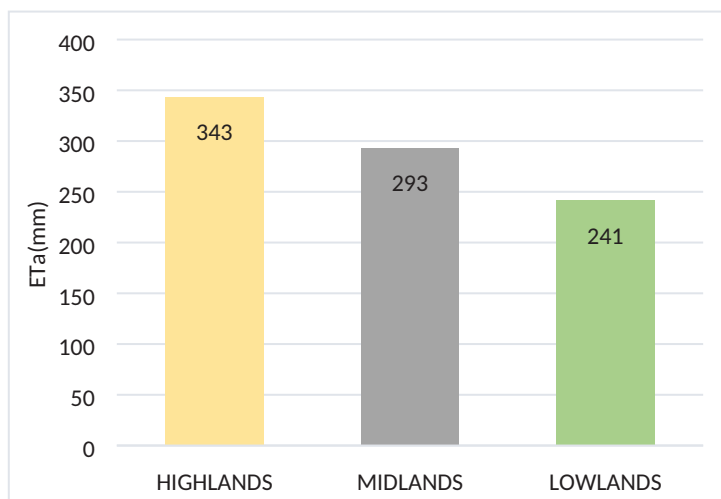
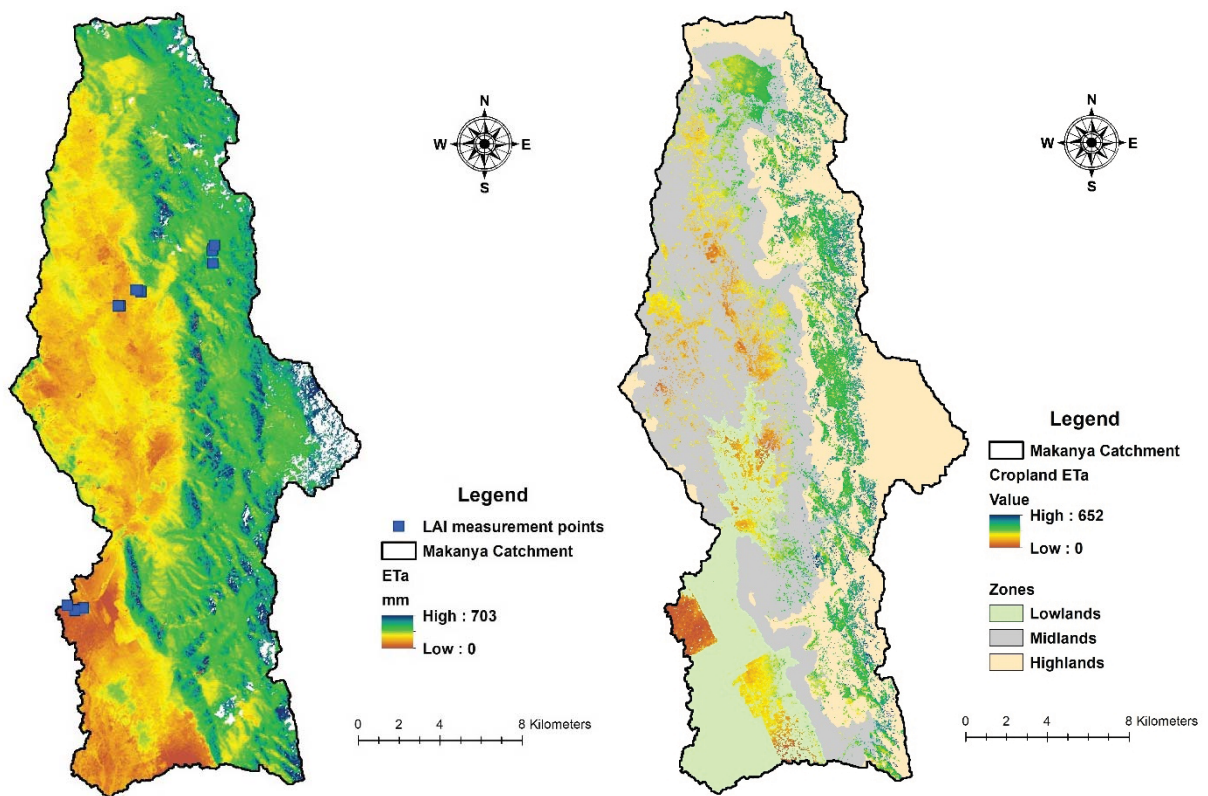


Figure 7. Average Seasonal ET_a for the agro-ecological zones

The average ET_a for the maize crop for the midlands season is lower than the crop water requirements of about 349 mm computed for the midlands using daily weather data for the areas. This indicates that the maize crop in the catchment is water stressed. Other factors that may have contributed to low ET_a were soil fertility, poor agricultural practices and pest/disease attack. Overall, the ET_a variations display a similar spatial trend as shown by yield, although in some parts of the catchment, especially in the midlands, relatively high ET_a is accompanied by low yield. Other than water stress, the high variability of ET_a estimates in the entire catchment may be attributed to other factors such as soil fertility and presence of trees on farms, high ET_a crops such as banana and coffee plantations. The agricultural block within the lowlands with very low ET_a had no crops growing during this season as farmer hardly farm these lands during this season. Therefore, the block had bare soils or very small stacks of naturally growing vegetation. During the long rains farmers in this agricultural block rely on rainfed agriculture and spate irrigation from flood water coming from the highland and midlands.

The three fields in the highlands (A, B and C) have comparable higher yields and higher actual ET than the ones in the midlands. This is because the highlands have been reported to receive higher amounts of rainfall than in the other parts of the catchment. Mean annual rainfall in Makanya catchment varies from 500 to 800 mm annually. The midland fields (D and E), although with supplementary irrigation, registered less ET_a . Based on the sampled fields, Field C registered the highest WP_{ET} because it attained the highest yields whereas field D registered the lowest WP_{ET} because of its low Biomass and subsequent low yields. Fields D and E were both under supplementary irrigating and under the same environmental conditions in the midlands, thereby reporting a slight difference in their Biomass, LAI and ET_a , and in turn a slight difference in the yields of the fields indicating that the two fields must have been under very similar field management practices.

WP_{ET} in the mid and lowland areas of Makanya catchment were very low when compared to global values as presented by Zwart & Bastiaanssen (2004), which range from 1.1 to 2.7 kg/m^3 and an earlier study by FAO which reported a range of 0.8 to 1.6 kg/m^3 (Doorenbos and Kassam, 1979). This is because of the low yields obtained in the mid and lowland areas of catchment. These results are comparable to earlier observations reported in the catchment by means of field observations by Makurira et al. (2011) who reported a range from 0.35 kg/m^3 to 0.51 kg/m^3 .

Similarly, studies by Mutiro et al. (2006) reported a range from 0.1 to 0.6 kg/m³ in these zones of Makanya catchment.

The Highlands however reported relatively higher WP_{ET} due to its higher suitability for maize farming as a result of the high rainfall and higher soil fertility in the zone.

Table 5. SEBAL/Sentinel-2 and field measurements on study plots at the late stage

Field	Location	Water application	SEBAL/Sentinel-2					Field
			Biomass (kg/ha)	ET _a (mm)	Yield (kg/ha)	WP _{ET} (kg/m ³)	LAI	LAI
A	Highlands	Rainfed	12,023	404	5,650	1.4	1.61	1.20
B	Highlands	Rainfed	13,130	409	6,171	1.5	1.86	1.46
C	Highlands	Irrigated	14,898	419	6,954	1.6	2.55	2.32
D	Midlands	Irrigated	4,955	337	2,329	0.6	1.20	1.20
E	Midlands	Irrigated	5,024	332	2,361	0.7	1.20	1.37

3.4 Crop Productivity (biomass production and yield)

The biomass production pattern over the entire catchment (Figure 8a) corresponds with the ET_a variation in the season (Figure 6a), whereby forested areas have the highest biomass production. The area that once was a wetland located in the lowest part of the catchment has the lowest ET_a and consequently low biomass production since the wetland is now dried up and covered with bare soils, sparse shrubs/ bushes.

The average biomass production for maize crops in the catchment over the season was 6804 kg/ha with values ranging from 0 kg/ha to 14796 kg/ha with the areas that reported no biomass being cultivated lands with no crops growing at the time of this study. The highest maize biomass production was achieved in the highlands, in the higher altitude parts of the midlands and in most of the areas located along the river course that benefitted from irrigation. The highlands have the highest average maize biomass production for the season with an average of 7583 kg/ha followed by the midland areas averaging 4311 kg/ha and lastly the lowland areas with 2766 kg/ha (Figure 9).

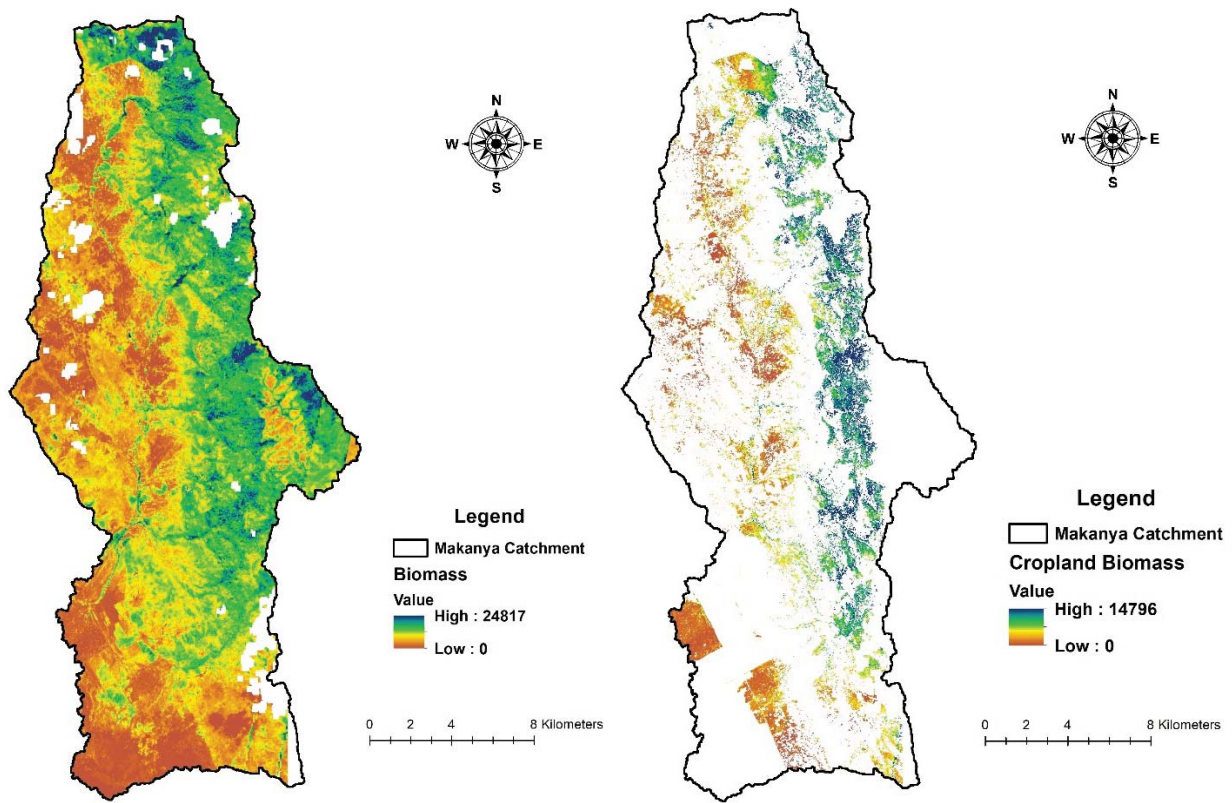


Figure 8. Seasonal biomass production a) for the entire catchment, and b) for the agricultural areas

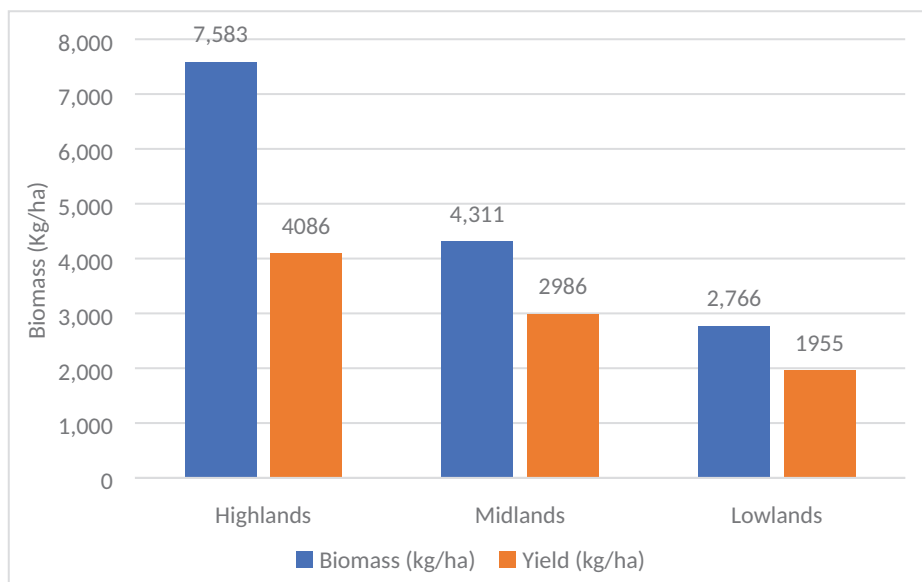


Figure 9. Average biomass and maize yield for the agro-ecological zones

The average maize yield for Makanya catchment for the season was 3171 kg/ha, with average yields attained in the highlands, midlands and lowland areas being 4086 kg/ha, 2986 kg/ha and 1955 kg/ha, respectively. It is also worth noting that the yields attained in each zone varied spatially.

During the field campaign, many farmers in the Makanya catchment reported getting yields ranging from 600kg/ha to 3000 kg/ha depending on the conditions for the season (mainly water availability and pests). The results from Sentinel-2 biomass and yield are within the range reported by farmers. These yields however do not reach their full potential of about 5000 kg/ha as reported by Mutiro et al. (2006) for the entire catchment. The average yield of 3171 kg/ha that was attained in the catchment during this season under study was higher than the typical maize yields of about 1000kg/ha reported by Makurira et al. (2011) and the yields of 1500 – 2000kg/ha reported by Kinoti et al (2010) in the various parts of Makanya Catchment.

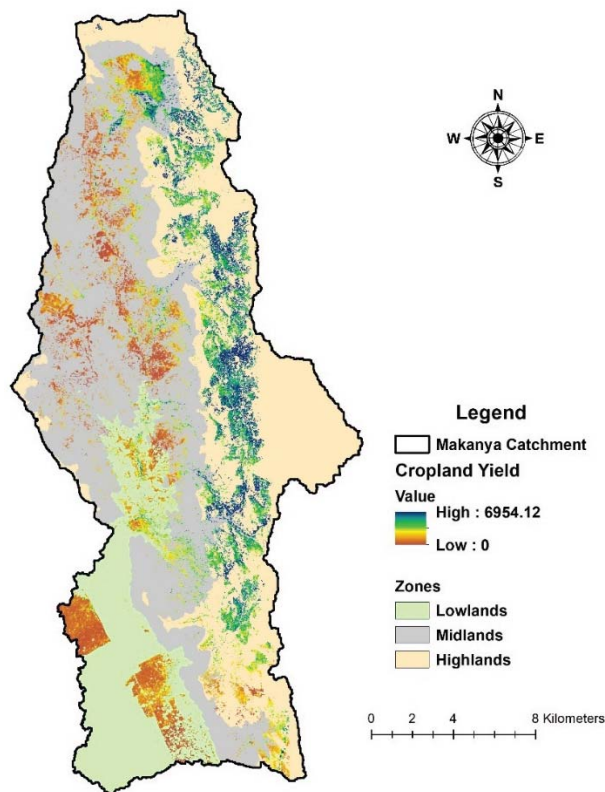


Figure 10. Agricultural yield map

3.5 Water Productivity

The average maize WP_{ET} in the Makanya catchment for the Vuli season was 0.79 kg/m^3 with values ranging from 0.00 kg/m^3 to 2.54 kg/m^3 with a standard deviation of 0.49 kg/m^3 (Figure 11). The values for the highlands, midlands and lowlands are 0.84 , 0.74 and 0.53 kg/m^3 , respectively (Figure 12). Figure 10 also shows that the WP_{ET} variation closely follows the pattern of yield variation in the area.

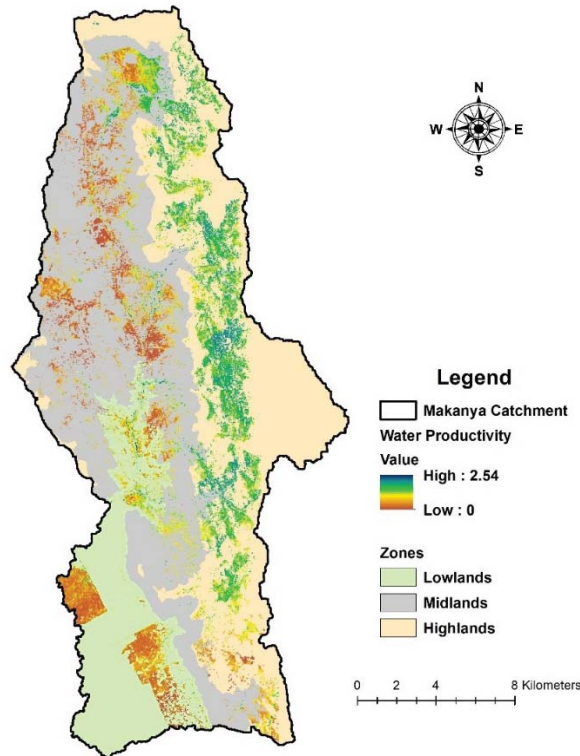


Figure 11. Water Productivity map

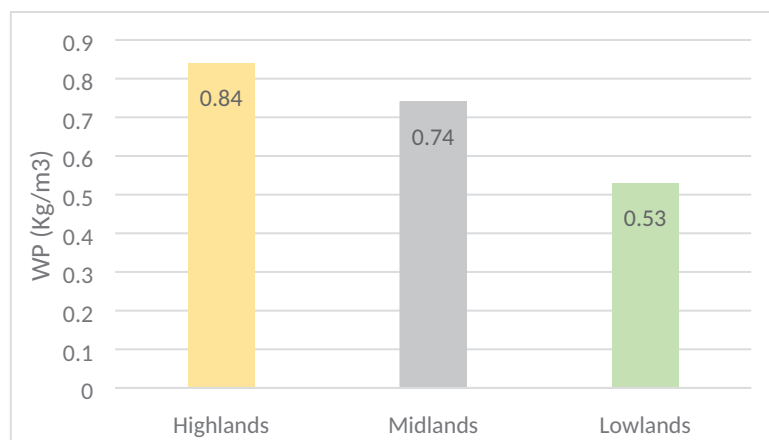


Figure 12. Average WP_{ET}

The results of ET_a , biomass, yield and WP_{ET} showed a clear negative gradient from the agricultural areas of highlands to lowlands in terms of actual ET and productivity. With the highlands, on average, receiving & consuming more water thereby producing more yield and the lowlands with the least seasonal water use as well as yields. In turn, the WP_{ET} in the highlands is higher than in the midlands and lowlands (producing more crop per drop). This may be attributed to inefficient and ineffective supplemental irrigation in the midland and lowland areas as the irrigation systems currently in place do not provide enough irrigation water mainly due to high conveyance losses along with significant losses through evaporation and runoff.

4. Conclusion and recommendation

In this study, we successfully demonstrated a coupled stepwise phenological variability-Supervised classification approach to generate high accuracy LULC layers. We also demonstrated the use of SEBAL and remote sensing data for WP_{ET} mapping in a cultivated African catchment. But, local information on land use, phenology and LAI are seen as essential inputs. Calibration of the remotely sensed LAI generated improved estimates of LAI that were within acceptable levels of errors and uncertainty reported in other similar studies. An innovative approach of Landsat-8 and Sentinel-2 data fusion was used that relied on LAI obtained from both satellite platforms supported with downscaling of RS biomass and yield thereby obtaining high-resolution and high accuracy biomass and yield estimates. Good estimates of ET_a from Landsat-8 were also obtained which together with yield were used to map the WP_{ET} in the catchment. Final estimates of WP_{ET} were within acceptable levels of uncertainty.

A comparative analysis of biomass, yield, ET_a , and WP_{ET} maps gives an indication that there is great potential for improvement in the WP_{ET} in the Makanya catchment especially in many parts of the midlands and lowland areas which exhibit the lowest WP_{ET} . This can be achieved by practicing field management techniques that reduce soil moisture loss through evaporation (e.g. mulching), reduce surface runoff (e.g., mulching and soil bunds), promote transpiration for biomass production (e.g. application of fertilizers, adapted varieties, weed control), and use the irrigation water more effectively (e.g. by timely application of the right quantity) so water stress can be reduced with the limited amount of irrigation water available.

Farmers in all parts of the catchment indicated lack of water as a major constraint to crop production and additionally pest attacking the crops were also listed by farmers as a major hindrance to high production. However, low WP_{ET} in many fields within the midland areas of the catchment can be attributed to poor irrigation practices, poor agricultural management practices and poor irrigation scheduling in most of the farms. High irrigation water losses is also rampant since the irrigation canals are unlined, un-gauged and manually controlled. Furthermore, there is no system to calculate the net water requirement for crops at a particular time for the areas that practice supplementary irrigation. With this system in place, it would promote the practice of deficit irrigation where application of the right quantities of this limited water resources would be done at the critical phenological stages of crop development such as the flowering stage. This system can go a long way in improving the yields in the catchment as well as improving the WP_{ET} . Since on average the seasonal water use of 331 mm is lower than the crop water requirement for the typical maize varieties in the area estimated as about being above 349 mm we infer that water stress is indeed a major constraint to crop productivity and consequently WP_{ET} . When a crop is water stressed at the critical stages of development (flowering), yields are considerably reduced irrespective of the amount of water applied in the later stages of development. This scenario is common in Makanya especially in the midland and lowlands. It's also important that farmers adopt smart agricultural management strategies aimed at conserving soil water as most of the unproductive water losses comes from evaporation from the soil.

As WP_{ET} is strongly related to water availability and weather conditions, the level of WP_{ET} may vary from season to season, year-to-year, even if field and water management practices are similar in all situations. We therefore recommend further analysis of WP_{ET} mapping over both *Vuli* and *Masika* seasons for different years.

Crop water use and WP_{ET} products can be further improved by developing better downscaling approaches from the Landsat products. Temporal resolutions can also be further improved by developing field-based models from field measurements. The model results can then be linked with remote sensing products for improved seasonal simulations. This involves field-based measurements, modeling and analysis throughout the season. There is need to also measure biomass and ET to support with validation of the RS products.

In this study, high resolution products of 10-meter resolution were developed that provided better representation of biomass, yield, water use and water productivity for small catchments. Future improvements in satellite product spatial and temporal resolutions are also expected to greatly contribute to better estimation and analysis of the spatial and temporal crop water use and WP_{ET} given the high spatial variability of African cultivated catchments.

Acknowledgements

We gratefully thank the TIGERBRIDGE project for the support. The opinions expressed herein are those of the author(s) and do not necessarily reflect views of TIGER-BRIDGE project. We also thank the Sustainable Management of Natural Resources by reducing Evapo-Transpiration in cultivated African catchments (SMART-ET) project funded by the VLIR-UOS fund of Flanders.

5. References

1. Ahmad, M. D., Biggs, T., Turrall, H., and Scott, C. A. (2006). Application of SEBAL approach and MODIS time-series to map vegetation water use patterns in the data scarce Krishna River Basin of India. *Water Science and Technology*, 53(10), 83-90. [doi:10.2166/wst.2006.301]
2. Allen, R. G., Pereira, L. S., Howell, T. A., & Jensen, M. E. (2011). Evapotranspiration information reporting: I. Factors governing measurement accuracy. *Agricultural Water Management*, 98(6), 899–920. <https://doi.org/10.1016/j.agwat.2010.12.015>
3. Allen, R., Irmak, A., Trezza, R., Hendrickx, J. M. H., Bastiaanssen, W., & Kjaersgaard, J. (2011). Satellite-based ET estimation in agriculture using SEBAL and METRIC. *Hydrological Processes*, 25(26), 4011–4027. <https://doi.org/10.1002/hyp.8408>
4. Andam-Akorful, S. A., Ferreira, V. G., Awange, J. L., Forootan, E., and He, X. F. (2014): Multi-model and multi-sensor estimations of evapotranspiration over the Volta Basin, West Africa, *International Journal of Climatology*, 35, 3132-3145.
5. Bastiaanssen, W. G. M., Menenti, M., Feddes, R. A., and Holtslag, A. A. M. (1998): The Surface Energy Balance Algorithm for Land (SEBAL): 1. Formulation, *J. of Hydrology*, 212-213 198-212.
6. Bastiaanssen, W.G.M.; Noordman, E.J.M.; Pelgrum, H.; Davids, G.; Thoreson, B.P.; Allen, R.G. SEBAL Model with remotely sensed data to improve water resources management under actual field conditions. *J. Irrig. Drain. Eng.* 2005, 131, 85–93.
7. Cai, A., Jia, L., van Opstal, J., Hessels, T., Bastiaanssen, W. (2017): Towards operational crop water productivity monitoring using remote sensing. IAHS2017-398, IAHS Scientific Assembly
8. Cai, X. L. and Sharma, B. R. (2010): Integrating remote sensing, census and weather data for an assessment of rice yield, water consumption and water productivity in the Indo-Gangetic river basin, *Agric. Water Manag.*, 97(2), 309–316.

9. Campbell G. S. (1986): Extinction coefficients for radiation in plant canopies calculated using an ellipsoidal inclination angle distribution. *Agricultural and Forest Meteorology* 36, 317–321.
10. Campbell, G.S. (1990): Derivation of an angle density function for canopies with ellipsoidal leaf angle distributions. *Agric. For. Meteorol.*, 49, 173–176
11. Choudhury, B. J., Ahmed, N. U., Idso, S. B., Reginato, R. J., and Daughtry, C. S. T. (1994): Relations between evaporation coefficients and vegetation indices studied by model simulations *Rem. Sens. Environ.*, 50, 1-17.
12. de Fraiture, C., Wichelns, D., Rockström, J. and Kemp-Benedict, E. (Editors), (2007): Looking ahead to 2050. Scenarios of alternative investment approaches, Chapter 3. IWMI, Colombo.
13. Doorenbos, J. and Kassam, A. H. (1979): Yield response to water, *Irrig. Drain. Pap.*, 33, 257.
14. Enfors, E. I. and Gordon, L. J. (2007): Analysing resilience in dryland agro-ecosystems: a case study of the Makanya catchment in Tanzania over the past 50 years, *Land Degrad. Dev.*, 18(6), 680–696.
15. Freitas, A. (2013): Water as a stress factor in -sub-Saharan Africa. In: EUISS Newsletter, 12, European Union Institute for Security Studies, Brussels Liaison Office.
16. Gascon, F.; Bouzinac, C.; Thépaut, O.; Jung, M.; Francesconi, B.; Louis, J.; Lonjou, V.; Lafrance, B.; Massera, S.; Gaudel-Vacaresse, A.; et al. Copernicus Sentinel-2A Calibration and Products Validation Status. *Remote Sens.* 2017, 9, 584. [CrossRef]Gerland, P., Raftery, A. E., Sevcíková, H., Li, N., Gu, D., Spoorenberg, T., Alkema, L., Fosdick, B. K., Chunn, J., Lalic, N., Bay, G., Buettner, T., Heilig, G. K., and Wilmoth, J. (2014): World population stabilization unlikely this century, *Science*, 346, 234-237.
17. Hessels, T., van Opstal, J., Trambauer, P., Bastiaanssen, W., Faouzi, M., Mohamed, Y., Er-Raji, A. (2017). pySEBAL version 3.3.7.
18. Jackson, R. D., Idso, S. B., Reginato, R. J., and Pinter, P. J. (1981): Canopy temperature as a crop water stress indicator *Water Resources Research* 17, 1133–1138.
19. Jackson, R. D. (1984): Remote sensing of vegetation characteristics for farm management, *SPIE Rem. Sens*, 475, 81–96.
20. Jarmain C and Meijninger Wl (2012): Assessing the impact of Invasive Alien Plants on South African water resources using remote sensing techniques. In: Neale CMU and Cosh MH (eds.) Proceedings of a Symposium organized by the International Commission on Remote sensing of IAHS, held at Jackson Hole, Wyoming, USA, 27-30 September 2010. IAHS Publication No. 352. IAHS Press, Oxfordshire. 388–392.
21. Jarmain C, Singels A, Obando E, Paraskevopoulos A and Mthembu I (2011) Water use efficiency of irrigated agricultural crops determined with satellite imagery. WRC Project No. K5/2079//4, Progress Report, December 2011. Water Research Commission, Pretoria.
22. Jarmain C, Singels A, Obando E, Paraskevopoulos A, Olivier F, Munch Z, Van Der Merwe B, Walker S, Van Der Laan M, Messehazion M, Savage M, Pretorius C, Annandale J and Everson C (2013): Water use efficiency of irrigated agricultural crops determined with satellite imagery. WRC Project No. K5/2079//4, Deliverable 6, Water Use Efficiency Report 2012/13, 15 January 2013. Water Research Commission, Pretoria.

23. Jensen, J. R. and Lulla, D. K. (1987): Introductory digital image processing: A remote sensing perspective, *Geocarto Int.*, 2(1), 65–65, doi:10.1080/10106048709354084.
24. Kääb, A.; Winsvold, S.H.; Altena, B.; Nuth, C.; Nagler, T.; Wuite, J. Glacier Remote Sensing Using Sentinel-2. Part I: Radiometric and Geometric Performance, and Application to Ice Velocity. *Remote Sens.* 2016, 8, 598.
25. Kijne, J. W., Barker, R., and Molden, D. J. (2003): Water productivity in agriculture; limits and opportunities for improvement: Comprehensive Assessment of Water Management in Agriculture Series No.1, edited by: International Water Management Institute, S. L., CABI Publishing, Wallingford.
26. Kinoti, J., Su, Z., Woldai, T. and Maathuis, B. (2010). Estimation of spatial-temporal rainfall distribution using remote sensing techniques: a case study of Makanya catchment, Tanzania. *International Journal of Applied Earth Observation and Geoinformation*, 12: S90–S99.
27. Kiptala, J. K., Mul, M. L., Mohamed, Y. A., and van der Zaag, P. (2014): Modelling stream flow and quantifying blue water using a modified STREAM model for a heterogeneous, highly utilized and data-scarce river basin in Africa, *Hydrology and Earth System Sciences*, 18, 2287-2303.
28. Kula, N., Haines, A., and Fryatt, R. (2013): Reducing Vulnerability to Climate Change in Sub-Saharan Africa: The Need for Better Evidence, *PLoS Med*, 10, e1001374.
29. MAFSC (2014): Agriculture Climate Resilience Plan 2014-2019, [online] Available from: <http://extwprlegs1.fao.org/docs/pdf/tan152483.pdf> (Accessed 27 May 2017).
30. Makurira, H., Savenije, H. H. G., Uhlenbrook, S., Rockström, J. and Senzanje, A. (2011): The effect of system innovations on water productivity in subsistence rainfed agricultural systems in semi-arid Tanzania, *Agric. Water Manag.*, 98(11), 1696–1703.
31. Makurira, H. (2010): Water Productivity in Rainfed Agriculture: UNESCO-IHE PhD Thesis, CRC Press.,.
32. Mancosu, N., Snyder, R. L., Kyriakakis, G. and Spano, D. (2015): Water scarcity and future challenges for food production, *Water*, 7(3), 975–992.
33. Mannschatz, T., Pflug, B., Borg, E., Feger, K. H., & Dietrich, P. (2014). Uncertainties of LAI estimation from satellite imaging due to atmospheric correction. *Remote Sensing of Environment*, 153, 24–39. <https://doi.org/10.1016/j.rse.2014.07.020>
34. Menenti, M., Visser, T. N. M., Morabito, J. A., and Drovandi, A. (1989): Appraisal of irrigation performance with satellite data and georeferenced information, in Rydzewski, J.R. and Ward, C.F. (eds.) *Irrigation, Theory and Practice*, Proc. of the Int. Conf., Institute of Irrigation Studies, Southampton, 12–15 September 1989: 785–801.,
35. Mul, M.L., (2009). Understanding hydrological processes in an ungauged catchment in sub-Saharan Africa. PhD Thesis, UNESCO-IHE, Delft, 130 pp.
36. Mul, M. L., Kemerink, J. S., Vyagusa, N. F., Mshana, M. G., Van der Zaag, P. and Makurira, H. (2011): Water allocation practices among smallholder farmers in the South Pare Mountains, Tanzania: The issue of scale, *Agric. Water Manag.*, 98(11), 1752–1760.
37. Mutiro, J., Makurira, H., Senzanje, A. and Mul, M. L. (2006): Water productivity analysis for smallholder rainfed systems: A case study of Makanya catchment, Tanzania, *Phys. Chem. Earth Parts ABC*, 31(15), 901–909.

38. Olofsson P, Giles M. Foody, Stephen V. Stehman c, Curtis E. Woodcock (2013). Making better use of accuracy data in land change studies: Estimating accuracy and area and quantifying uncertainty using stratified estimation. *Remote Sensing of Environment* 129:122–131.
39. Perry, C., Pasquale, S., Allen, R. G., and Burt, C. M. (2009): Increasing productivity in irrigated agriculture: agronomic constraints and hydrological realities *Agricultural Water Management* 96, 1517–1524.
40. Pickering, A. J., and Davis, J. (2012): Freshwater Availability and Water Fetching Distance Affect Child Health in Sub-Saharan Africa, *Environmental Science and Technology*, 46, 2391-2397.
41. Rango, A., and Shalaby, A. (1998): Operational applications of remote sensing in hydrology success prospects and problems *IAHS Hydrol. Sci. J.*, 43, 947-968.
42. Richardson, A. D., Dail, D. B., & Hollinger, D. Y. (2011). Leaf area index uncertainty estimates for model-data fusion applications. *Agricultural and Forest Meteorology*, 151(9), 1287–1292. <https://doi.org/10.1016/j.agrformet.2011.05.009>
43. Rockström, J., and Falkenmark, M. (2015): Agriculture: Increase water harvesting in Africa, *Nature*, 519, 283-285.
44. Singh, R. K., Irmak, A., Irmak, S. and Martin, D. L. (2008): Application of SEBAL model for mapping evapotranspiration and estimating surface energy fluxes in south-central Nebraska, *J. Irrig. Drain. Eng.*, 134(3), 273–285.
45. Stewart, J. B., Watts, C. J., Rodriguez, J. C., de Bruin, H. A. R., van de Berg, A. R., and Garatuza-Payan, J. (1999): Use of satellite data to estimate radiation and evaporation for northwest Mexico, *Agric. Wat. Manage*, 38, 181-193.
46. Su, Z., (2002): The Surface Energy Balance System (SEBS) for estimation of turbulent heat fluxes. *Hydrol. Earth Syst. Sci.* 6, 85–99.
47. Till, M. R., and Bos, M. G. (1985): The Influence of Uniformity and Leaching on the Field Application Efficiency In: *ICID Bulletin*, New Delhi.
48. URT, U. R. o. T. (2007): *Poverty and Human Development Report 2007*, Dar es Salaam, Tanzania.
49. Webb, N., Nicholl, C., Wood, J., & Potter, E. (2016): *SunScan Manual version 3.3*, 1–82.
50. Zwart, S. J. and Bastiaanssen, W. G. (2004): Review of measured crop water productivity values for irrigated wheat, rice, cotton and maize, *Agric. Water Manag.*, 69(2), 115–133.
51. Zwart, S. J., Bastiaanssen, W. G., de Fraiture, C. and Molden, D. J. (2010): WATPRO: A remote sensing-based model for mapping water productivity of wheat, *Agric. Water Manag.*, 97(10), 1628–1636.